LCC-0065
June 2001

Linear Collider Collaboration Tech Notes

NLC Positron Target Heating

D. C. Schultz, Y. K. Batygin, V. K. Bharadwaj, J.C. Sheppard

Stanford Linear Accelerator Center
Stanford, CA

Abstract: The NLC requires an intense beam with a large number of positrons. These positrons are produced by a high energy electron beam impinging on a solid tungsten-rhenium alloy target. The particle shower that develops in the solid target deposits significant energy in the material, leading to target stresses and potentially to target damage. The stresses can be analyzed once the magnitude and extent of the energy deposition is known. This note details the modeling of the energy deposition using EGS, performed for the NLC and the SLC targets and for possible NLC targets made of copper or nickel instead of WRe.

NLC Positron Target Heating

David C. Schultz, Yuri K. Batygin, Vinod K. Bharadwaj, John C. Sheppard
Stanford Linear Accelerator Center, Stanford University, CA 94309

June 19, 2001

Abstract:

The NLC requires an intense beam with a large number of positrons. These positrons are produced by a high energy electron beam impinging on a solid tungsten-rhenium alloy target. The particle shower that develops in the solid target deposits significant energy in the material, leading to target stresses and potentially to target damage. The stresses can be analyzed once the magnitude and extent of the energy deposition is known. This note details the modeling of the energy deposition using EGS, performed for the NLC and the SLC targets and for possible NLC targets made of copper or nickel instead of WRe.

Introduction:

The positron beam for the NLC beam is generated using a 6.2 GeV electron beam impinging on a solid Tungsten Rhenium target. The positrons produced at the target occupy a large phase space and must be damped in a pre-damping ring for injection into the main damping ring. The properties of the positron beam at the entrance to the pre-damping ring are listed below. There are two running configurations one with 190 bunches per train and the other with 95 bunches per train.

Energy	E	1.98	1.98	GeV
Accepted emittance (norm. edge)	?e	0.03	0.03	m-rad
Number of bunches	N_b	190	95	#
Positrons/bunch	n_B	0.9	1.8	10^{10} positrons
Bunch spacing	T_b	1.4	2.8	ns
Repetition rate	f	120	120	Hz

The required high intensity of positrons leads to high energy deposition in the positron target. To examine the peak energy deposition in targets and the volume of the targets where the energy is deposited, several EGS [1] runs were performed of specific positron target cases: for the standard NLC WRe[1] target, for the SLC WRe target, and for potential Cu and Ni NLC targets. Details of these target configurations are given in the table below. The results of the analysis are summarized in this note.

[1] W25Re, an alloy of 75% Tungsten with 25% Rhenium, was used in the simulation as this material is readily available in the EGS database.

Case	Target material	Rad. Len.	e^- beam energy	e^- beam pop.	e^- beam sigma
SLC	6RL W25Re	3.43 mm	33 GeV	1 x $4x10^{10}$	0.8 mm
NLC	4RL W25Re	3.43 mm	6.2 GeV	95 x $1x10^{10}$	1.6 mm
NCL-Cu	4RL Copper	14.40 mm	6.2 GeV	95 x $1x10^{10}$	1.0 mm
NCL-Ni	4RL Nickel	14.25 mm	6.2 GeV	95 x $1x10^{10}$	1.0 mm

Peak energy deposition:

The geometry in EGS was set up to sum the energy deposited in a 1mm diameter cylinder in the center of the target, running the length of the target, placed with the cylinder axis parallel to the beam direction and with x=y=0 (z is the cylinder center line). This center volume of the target is where the energy deposition is highest, and as the electron beam spot size has $s_r \geq 1$ mm the energy deposited in this volume should be reasonably[2] uniform radially. The remaining outer volume of the target was present in the simulation but treated as a separate EGS volume. The incoming electron beam in EGS had $s_x = s_y = 0$, y=0, a different x for each EGS run, dx/dz=dy/dz=0, and an energy specific to the case in study (see table). As a shower develops at a distance x away from the center of the cylinder the energy deposited in the target can be inside or outside the central 1mm diameter volume. The EGS analysis gives (EDEP*WT(NP)/ TotKE0) the fraction of incoming beam energy deposited in the central 1mm diameter volume of the target between a depth of z and z+dz (dz being the size of an EGS histogram bin). Many EGS runs were made for each specific case in study, with different values of x for each EGS run. The histograms of the energy deposited in the center of the target (vs. z) can then be convoluted with the electron beam gaussian radial profile for the specific case in study.

For each specific case in study, with the EGS results in hand for a number of beam-centerline-to-target-centerline separations x_i, the following sum is made.

$$\frac{J}{g}(z) = E_0 / s^2 \times \sum_i dE_i(z) \times r_i dr_i \times \exp\left[r_i^2 / 2s^2\right] / m_i$$

with; $J/g(z)$ = Joules per gram in the target at a depth z
E_0 = the incoming beam energy per bunch train,
s = the incoming electron beam sigma,
dE_i = the fraction of energy deposited (from EGS) in the central target volume at (z, z+dz), from the i_{th} value of x,
r_i = the i_{th} value of x, taken as a radius in the electron beam's radial distribution,
$dr_i = \frac{1}{2}(x_{i+1}+x_i) - \frac{1}{2}(x_i+x_{i-1})$
and m_i = the mass of the 1mm diameter central target volume between z and z+dz.

The results of the summation are plotted below

[2] Integrating a gaussian out to 0.5 mm, the peak energy deposition should be approximately 3%, 6% and 9% higher for 1.6 mm, 1.0 mm and 0.8 mm s_r electron beams.

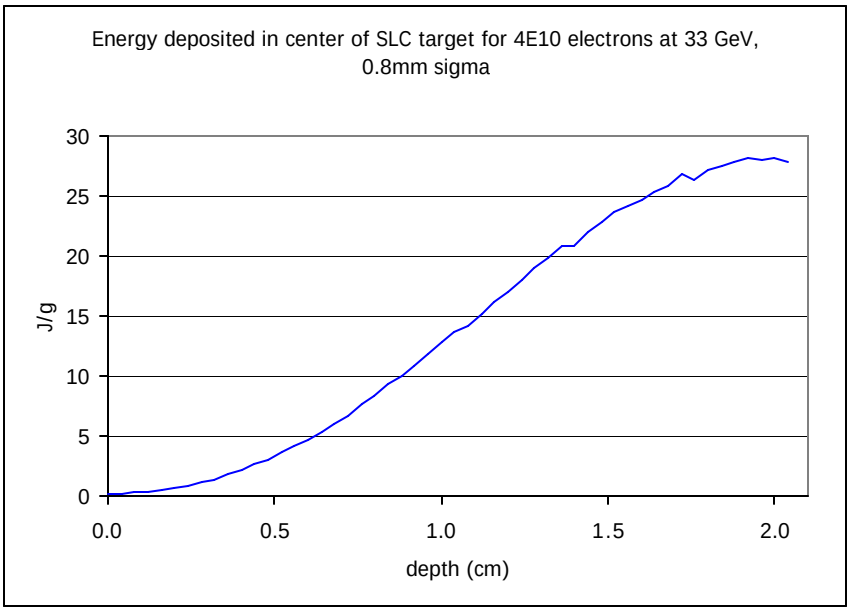

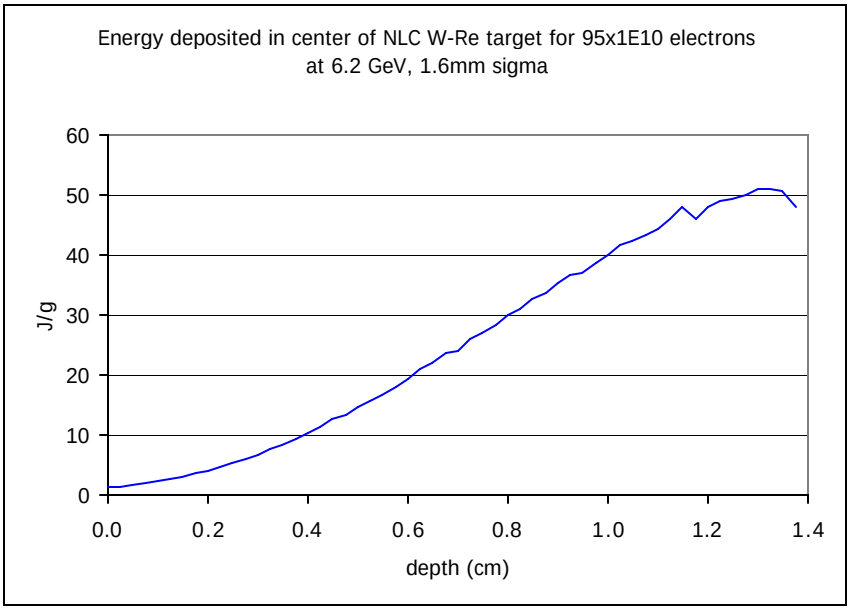

The plots show slight anomalies in the deposited energy at z ~ 1.7, 1.4, 1.1, … cm. These are an artifact of the way the volumes in EGS were set up, and can be ignored.

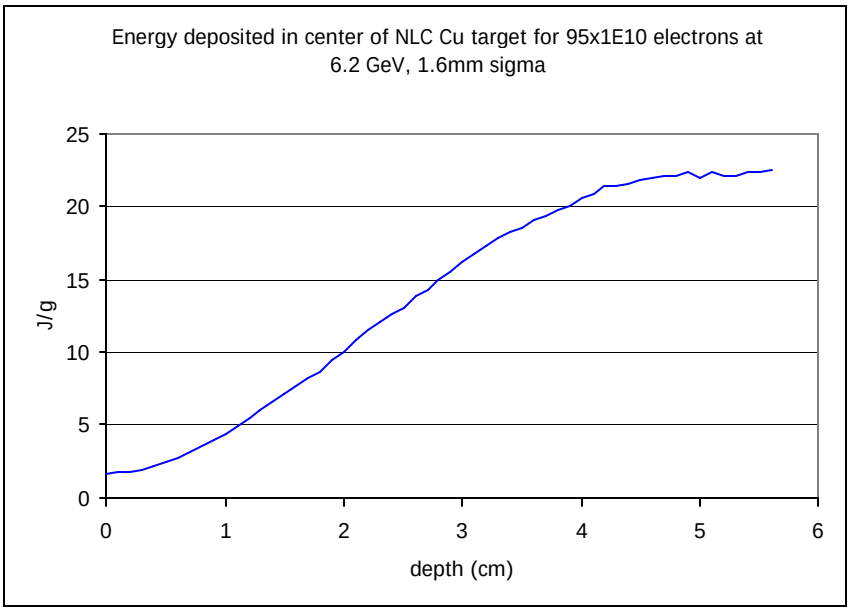
Energy deposited in center of NLC Cu target for 95x1E10 electrons at 6.2 GeV, 1.6mm sigma
J/g
25
20
15
10
5
0
0
1
2
3
4
5
6
depth (cm)

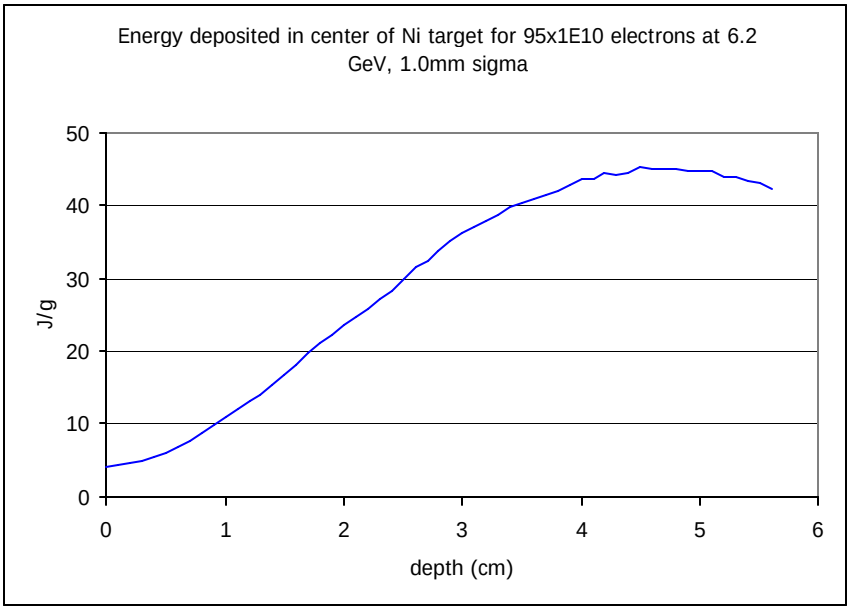
Energy deposited in center of Ni target for 95x1E10 electrons at 6.2 GeV, 1.0mm sigma
J/g
50
40
30
20
10
0
0
1
2
3
4
5
6
depth (cm)

The results are summarized in this table, and compared to other analyses:

Normalized comparison:						scaled J/g max
This note	SLC	6RL W25Re	33 GeV	1 x $4x10^{10}$	0.8 mm	28
AK [2]	SLC	6RL W25Re	33 GeV	1 x $4x10^{10}$	0.8 mm	30
This note	NLC	4RL W25Re	6.2 GeV	95 x $1x10^{10}$	1.6 mm	52
TK [3]	NLC	4RL W25Re	6.2 GeV	95 x $1.0x10^{10}$	1.6 mm	50
Mokhov [4]	NLC	4RL W25Re	6.2 GeV	95 x $1.0x10^{10}$	1.6 mm	51
This note	NCL-Cu	4RL Copper	6.2 GeV	95 x $1x10^{10}$	1.0 mm	43
This note	NCL-Cu	4RL Copper	6.2 GeV	95 x $1x10^{10}$	1.6 mm	22
Mokhov	NCL-Cu	4RL Copper	6.2 GeV	95 x $1.0x10^{10}$	1.6 mm	25
This note	NCL-Ni	4RL Nickel	6.2 GeV	95 x $1x10^{10}$	1.0 mm	45

Shower size:

The table above gives the maximum energy deposition in the target, but does not address the volume of the target over which this energy is deposited. To examine the radial extent of the energy deposition EGS was again used. The EGS geometry was set up to sum the net energy deposition in each of nine concentric rings of constant radial width, for the last 0.10mm (0.26mm) of the $W_{25}Re$ (Cu, Ni) target in the table above. The results of this study are shown in the following graph.

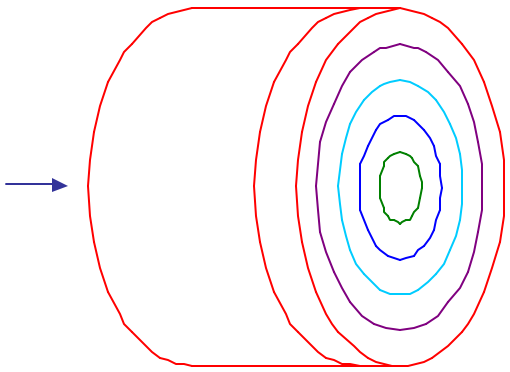

EGS setup of concentric rings in the target

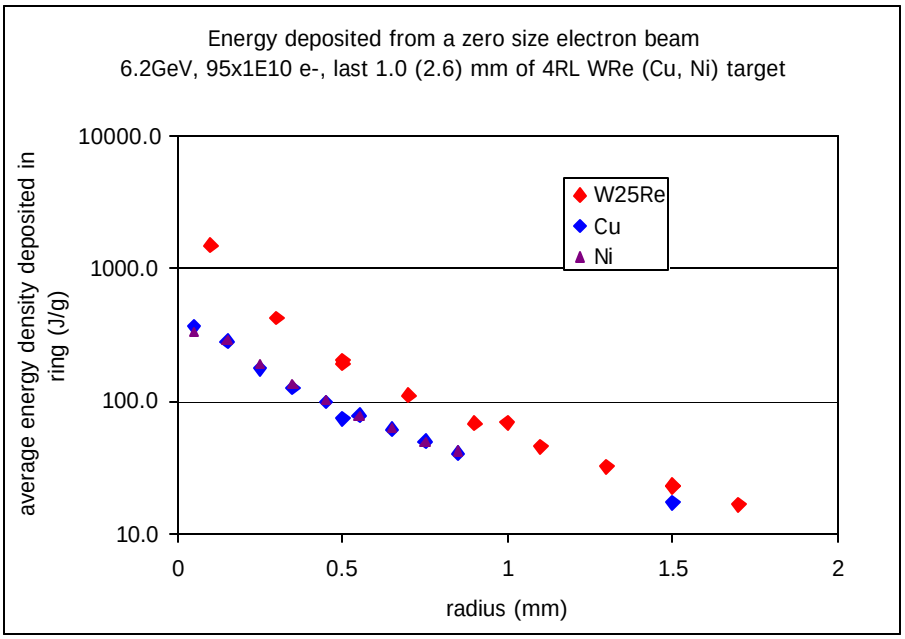

The radial distributions thus collected were convoluted with gaussian radial electron beam shapes. The 'energy density sigma' shown in the table below is half of the two-sigma point of this convoluted shape.

	target	E beam	e^- beam sigma	energy density sigma	growth*
NLC	4RL W25Re	6.2 GeV	1.6 mm	1.62 mm	.25 mm
NCL-Cu	4RL Copper	6.2 GeV	1.0 mm	1.04 mm	.29 mm
NCL-Ni	4RL Nickel	6.2 GeV	1.0 mm	1.04 mm	.27 mm

*growth=(energy density sigma^2 - e^- beam sigma^2)$^{1/2}$

NLC configuration:

Yuri Batygin's yield analysis using the code Beampath [5] gives a yield of 0.76 e^+/e^-. With 1.8×10^{10} e^+ needed at the PPDR in each of the 95 bunches in a train, 2.37×10^{10} e^- in each electron bunch will be needed.

EGS4 was run for a monoenergetic 6.2 GeV electron beam, counting the number of positrons at various depths of WRe, Cu and Ni targets. The results are shown in the following plot.

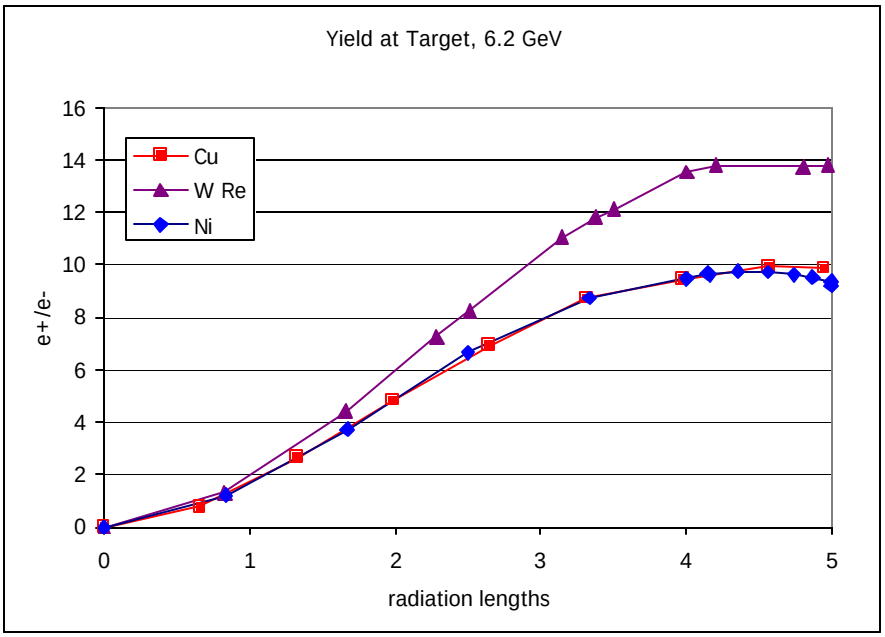

The plot shows the number of positrons increasing until a thickness of ~4 radiation lengths is reached. At 4 RL the Cu (Ni) yield (the yield shown in the plot above is e+/e- at the target surface) is 9.46 (9.47), while the WRe yield under the same conditions is 13.54. An EGS run was then done with a 4 RL Cu target to generate an input file for the Beampath yield analysis. Using a 1 mm sigma radius incident electron beam, the analysis gives a yield at the 250 MeV point of 1.15 e+/e- into a 0.03m-rad acceptance. This can be compared to a yield of 1.6 for a W Re target with an NLC standard 1.6 mm sigma electron beam. The yield for Cu is 72% of that for W Re.

The net yield is still under study and may improve. The relative yield, WRe vs. Cu should also change as the yield studies advance.

NLC configurations:					scaled J/g max	note:
NLC	4RL W25Re	6.2 GeV	95 x 2.4×10^{10}	1.6 mm	125	1
NCL-Cu	4RL Copper	6.2 GeV	95 x 3.3×10^{10}	1 mm	143	2
NCL-Ni	4RL Copper	6.2 GeV	95 x 3.3×10^{10}	1 mm	149	3

1) Using a Yield of 0.76 with 1.8E10 e^+ needed at the PPDR
2) Using a Yield 1.15/1.6=.72 of that for WRe, 2.4*1.6/1.15=3.3
3) Using the same Yield as for Cu

Options:

There are several ways in which the peak energy deposition in the target can be reduced. For example, the electron beam spot size can be increased. The following figure shows the dependence of the yield (from Beampath) on the spot size.

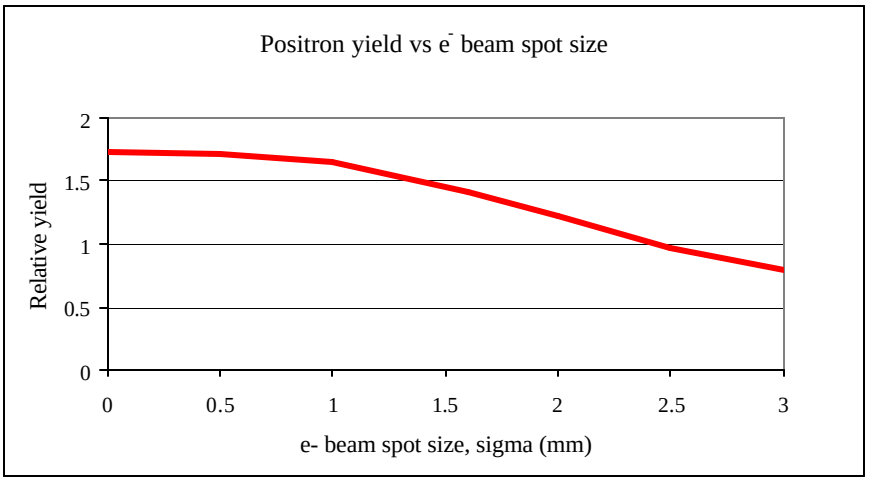

As the beam sigma is increased from 1.6 to 3 mm, the yield drops ~½ while the energy density drops ~¼. The stress in the target would be reduced at the cost of additional electron beam power. This cost-benefit optimization has not yet been done.

References:

[1] The EGS4 Code System, Nelson, Hirayama and Rogers, SLAC-265, Dec 1985.
[2] A. Kulikov, private communication
[3] from an earlier NLC analysis by T. Kotseroglou
[4] Krivosheev, Makhov and Striganov, Fermilab-TM-1965
[5] See Y. Batygin *et al*, in the PAC 2001 proceedings